UNIVERSITAT POLITÈCNICA DE CATALUNYA
BARCELONATECH
Escola Politècnica Superior d'Enginyeria de Manresa

Valorization of fines from construction and demolition wastes

Master's degree of Natural resources engineering

"Universidad Politecnica de Catalunya"

Cristobal Sebastian Bahamonde Padilla

Directores:

Maria Pura Alfonso Abella

Maria Teresa García Vallès

Index

Abstract

Circular economy is a concept and a new paradigm, it has been the base of the norms and laws that sustain the new practices on waste management in the countries that belong the European Union. Concept that is stronger nowadays, triggered by the climate crisis that is a fact and disturbing reality. Due to this, by 2020 the waste management sector had planned to valorize up to 75% of the construction and demolition waste(C&DW). The construction is a sector that not only produce waste on the construction and demolition activities, but also in the production of its main raw material. Portland cement manufactured cause 8% of the worldwide carbon dioxide emissions, with a total CO_2 emission of more than 2.5 Gt. Mainly produced by the calcination of the limestone in the clinker production.

The last report given by the waste management sector in 2021, showed that it has valorized 61,4% of the construction and demolition waste by 2020, value way below the main objective accorded. So, in the need to improve this performance, reduce the carbon footprint and slow down, or hopefully eventually stop the high exploitation of industrial minerals as limestone. The present article focuses on the characterization and valorization of two different fine aggregate waste that are product of the recycling process of the construction and demolition waste.

The fine aggregate is treated in the recycling plants and forms a silt that has had no economic interest. Due this, the thermal (DTA/TG), plastic, chemical (XRF) and mineralogic (XRD and SEM/EDS) properties of this materials has been studied to assess their potential use as partial replacement of Portland cement. Showing that the materials has high reactivity mostly due the roll of the C-S-H gel once it is thermally treated at 900°C. If at least 30% of replacement is carried out, the reduction of the C&DW stockpiled will allow that 77% of the C&DW be valorized. Bringing with it a reduction close to 451.000 tons of CO_2. Achieving the valorization goals of the industry, reducing the limestone exploitation and the carbon dioxide emissions.

Resumen

La economía circular es un concepto y un nuevo paradigma, ha sido la base de las normas y leyes que sustentan las nuevas prácticas sobre el manejo de residuos en los países que pertenecen a la Unión Europea. Concepto que hoy en día cobra más fuerza, desencadenado por la crisis climática que se ha convertido en un hecho y una realidad inquietante. Por ello, para 2020 en Catalunya, los gestores de residuos tenían previsto valorizar hasta el 75% de los residuos de construcción y demolición (RCD). Siendo el sector de la construcción, un sector que no solo produce residuos en las actividades de construcción y demolición, sino también en la producción de sus principales materias primas. El cemento Portland fabricado causa el 8% de las emisiones mundiales de dióxido de carbono, con una emisión total de CO2 de más de 2,5 Gt. Producido principalmente por la calcinación de la piedra caliza en la producción de Clinker.

El último informe entregado por el sector de la gestión de residuos en 2021, mostró que se ha valorizado el 61,4% de los residuos de construcción y demolición para 2020. Valor muy por debajo del objetivo principal acordado. Así que, en la necesidad de mejorar este desempeño, reducir la huella de carbono y frenar eventualmente la alta explotación de minerales industriales como la caliza. El presente artículo se centra en la caracterización y valorización de dos residuos de árido fino procedentes del proceso de reciclado de los residuos de construcción y demolición.

El árido fino es tratado en las plantas de reciclaje y forma un limo que no ha despertado interés económico en el último tiempo. Debido a esto, se han estudiado las propiedades térmicas (DTA/TG), plásticas, químicas (XRF) y mineralógicas (XRD y SEM/EDS) de estos materiales para evaluar su potencial uso como reemplazo parcial del cemento Portland. Demostrando que los materiales tienen una alta reactividad debido principalmente al rol del gel C-S-H una vez que es tratado térmicamente a 900°C. Si se realiza al menos un 30% de reposición, la reducción de los RCD almacenados permitirá que se valorice el 77% de estos. Trayendo consigo una reducción cercana a las 451.000 toneladas de CO2. Consiguiendo de esta manera cumplir con los objetivos de valorización de la industria, en conjunto con reducir la explotación de caliza y las emisiones de dióxido de carbono.

Introduction

Society has been growing at an unexpected pace during the last couple of centuries. After the period of colonization and as a consequence of the industrial revolution, the advance on mass production and globalization has created a world hyperconnected and with a strong sense of consumerism, all this has been backed up by the western philosophies and the idea of create a better world using the insatiable craving of development alongside the unstoppable system of free market and modern capitalism, system that had brought unification, connectivity and technological advances at a high human (genocides, proxy wars and inequality) and environmental costs.

This sense of technological development and economic growth developed during the XX century, brought with them a diversity of sources of anthropogenic pollution, the deforestation for cropping and cattle has destroyed important volume of tropical forest that are one of the main carbon sinks alongside the boreal forest (Schimel, 1995; Friedlingstein et al, 2021) and big sources of biodiversity. However, this development was linked to the surface water and groundwater pollution due to infiltration of hydrocarbons, nitrates/nitrites (Biddau, et al, 2019) and any toxic compound from different kind of industries, which impair the main sources of water in a moment of climate crisis and droughts.

All these different facts, among others, produced an elevated amount of greenhouse gasses, that brought as a consequence the rise of the atmospheric temperature. This effect started to be perceived and recorded by the humanity during the first half of the decade of the 70s (Coumou, and Rahmstorf et al, 2012), being the theory of global warming accepted by the end of the 80s, mainly due the many economic and political crises lived during the cold war, crises that empower the idea of self-sufficiency in some extent, especially on energy production. After this, countless attempts to find new and alternative sources of energy without the use of fossil fuels have been developed. So, despite the reactivity of the society in face of a problem, it has led it to be constantly looking for quick solutions in short periods of time, to problems caused by their own lack of environmental judgment.

The construction industry growth comes together with the success of the structured social systems (not necessarily good for everybody) and the development of new technologies, larger cities and the edification of new infrastructures are needed, thus this segment has become an important link in the emission of pollutants in two phases of its production chain. This development leads to an increased need for cement and concrete, which results in an increase in waste generated when buildings are modified or destroyed. The world production of cement exceeds 30 billion tons per year (Sousa et al, 2023). A significant amount of this is used to produce concrete, with an estimated production of 4.3 billion tons per year (Marvila et al, 2022). Portland cement (PC). The manufactured of the clinker, produce between 5-8% of the anthropogenic carbon dioxide emission worldwide

(Andrew, 2019), with a total CO_2 emission of more than 2.5 Gt (de Grazia et al, 2023). The calcareous raw material used during the thermal treatment to produce clinker has to be calcined at 800-900 °C; during this process calcite (calcium carbonate) is decomposed into lime and CO_2.

Nowadays this topic is a big concern for the scientific and industrial community, who is trying to figure out how to create an alternative cementitious material with less carbon emission.

In this sense, the circular economy has been the new solution to the waste management problem, being a policy that started to be accepted and pursued. The use of waste will avoid large concentrations of waste and the possible environmental contamination resulting from it. It will also reduce the need to extract raw materials from nature.

Given that modern society is facing numerous problems related with the anthropogenic pollutants. The present research has focused on one problem that has gone unnoticed in the public opinion, but it is an important source of CO2 emissions, as it is, the production of Portland cement.

The waste manager sector from Catalonia reported that 40,6% of the waste from the recycled plants are construction and demolition waste, C&DW (Agència de residus de Catalunya, 2021a) (Annex 1). 40 -50% of the fine particles generated had no apparent use (Contreras et al, 2016), being just the particles bigger than 5 mm the ones used as a replacement of coarse aggregate in concrete production.

In 2020 the amount of C&DW was around 6,7 million tons (Mt), 38.6% of it has been stockpile in controlled landfills, being 61.4% of the remained waste, subjected to a waste valorization process (Agència de residus de Catalunya, 2021b). Considering this last point, by 2020, around 2,6 Mt of the C&DW corresponds to fine powder that could be valorized being used as supplementary cement material (SCM). Previous research used the fine fraction of RC&D materials to the production of new clinker (Gastaldi et al, 2015; Zhutovsky and Shishkin, 2021). In other cases, they are used as supplementary cementitious materials (Tang et al, 2020; Li et al, 2022; Zhang et al, 2022).

From historical data of the cementitious industry given by the Ministry of industry and commerce of Spain, it is observed that just after the economic crisis of the 2009, the values of production of concrete and apparent consumption in Catalunya had dropped, and from 2013 onwards it was going through an economic stagnation with an average cement production of 2,8 Mt (Ministerio de Industria y comercio, 2021) (Annex 2). Nowadays, the last report of 2021, shows that 3,4 Mt of cementitious material was produced in Catalunya (18% more than the average) that supposed a yearly emission of 2,7 million of tons of CO_2.

This research aim to assess the opportunity to reduce the carbon footprint of the cement industry and the amount of waste generated by the construction industry, two sources of pollution related to the C&DW management, determining the characterization of the silt paste obtained from

the fine particles recycling that come from the crushing process of the C&DW, finding out a way to use it as a total or partial replacement of Portland cement production.

Methodology

For the present research, material from two different concrete recycling plants from Barcelona area in Catalunya were collected. The samples were basically two different materials from construction and demolition waste (C&DW), both materials come from the fine particle residue generated by the crushing process of the C&DW to obtain recycling concrete aggregate in the recycling plant. This waste is treated in a wet cycle, where this material passes through sedimentation using an organic flocculant (the additive description was not given by the company) to accelerate the precipitation of the powder.

One of the samples is composed just by concrete aggregate residual fine particles (FC), other sample comes from a mix of concrete, clay bricks and other inorganic materials (FM). The third sample of non-treated concrete waste (CW) the material of size fraction under 63 μm of the C&DW.

These materials were tested through different analyses, checking its chemical and mineral composition, particle size, behaviour during a thermal treatment, plasticity and pozzolanic reactivity. All these data are necessary to understand the basic properties of those materials and its potential use as supplementary cement material (SCM) once it is thermally treated.

Source and potential minerals found on recycled materials

As a common and more suitable spot for urbanized areas in Catalunya, specifically in Barcelona and surroundings, the settlement has been typically built up all over the depressions. The recycling plant is close to the cities of Barcelona, Sabadell and Terrassa. Barcelona is located in the Plana de Barcelona basin, which is mainly constituted of Quaternary detrital sediments. Sabadell and Terrassa or valleys near the main basins are located in the Vallès Depression. This depression is constituted mainly by Tertiary and Quaternary sediments, clays and also carbonate rocks from the Mesozoic age, with minor amounts of granitic rocks from the Prelitoral and Littoral Coastal ranges (Figure 1). Then, most of the material that constitutes the soils that are removed together with the construction materials has sedimentary origin and it can contain a certain amount of limestones and dolostones.

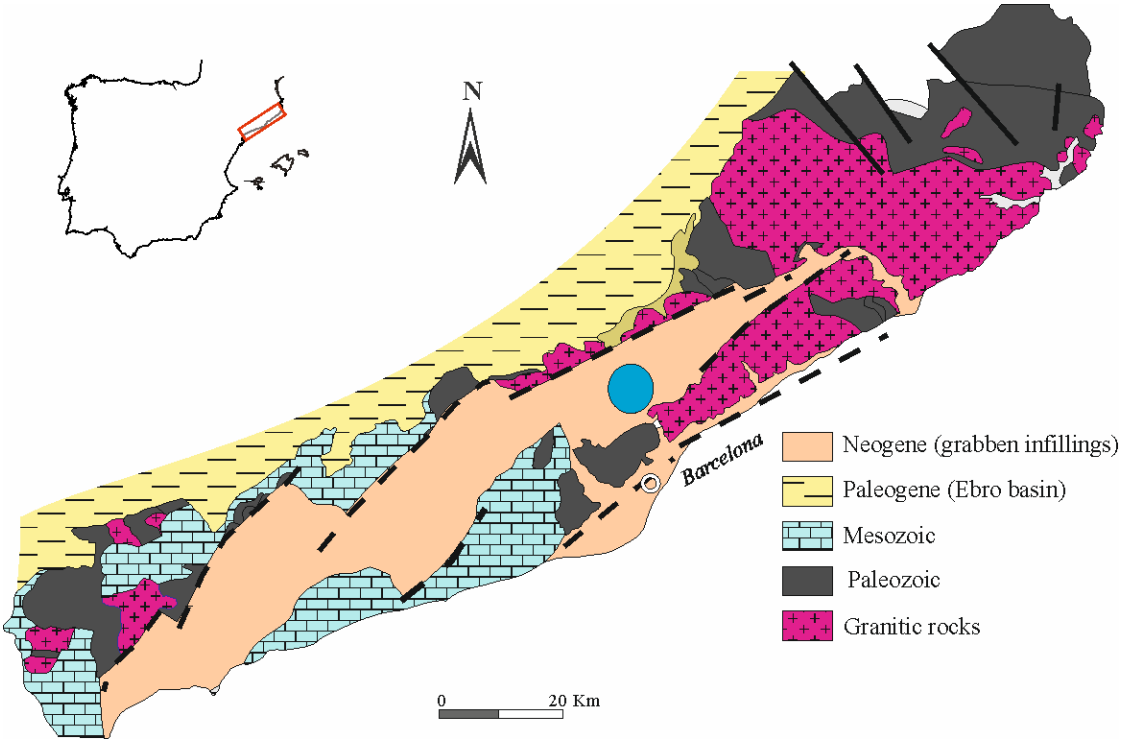

Figure 1. Geological map of the east of Catalonia, with the location of the recycling plants (brue dot).

The materials used are the finest fraction of the recycled C&DW. The recycling plants normally use a water recycling system in which particles of the silt and clay fraction (<63 μm) are removed by sedimentation with the addition of flocculant. These finer particles are separated from the wastewater by filtration and pressing. Typical CDW washing plants produce a silt filter cake of between 5 and 80 tonnes per hour, depending on the size of the plant and the materials being processed. This waste is usually landfilled. Given the large amount of residual sludge produced, together with the transport and decreasing landfill space, sludge disposal is becoming a major problem.

Particle size distribution

The particle size distribution of the raw materials has been determined by means of a LS 13 320 Coulter particle size analyser (Beckman, Brea, CA, USA). Before being measured, the samples were treated with sodium pyrophosphate and agitated mechanically for 24 h in order to achieve a total disaggregation.

For this account, the material was quartered to obtain a representative sample and placed on a sample vial. From this vial was taken a small amount to mix it with sodium pyrophosphate which is used as chemical dispersant. This process was executed for the original samples, the samples that

were grinded with the ball mill and the samples grinded with the disk mill, for the last one, an extra sample was added to the process, which was a concrete waste without the organic flocculant used during the sedimentation in the recycling facility, to observe the differences that could cause the application of the additive on the mechanical treatment and particle size.

Chemical composition and thermal analysis

To determine the chemical composition of the sample the X- ray fluorescence (XRF) analysis was performed with an Epsilon 1 equipment of Malvern Panalytical company, detecting from Na to Am. For this account, the samples were dried out until 85-90 ◦ C during a period of 24 hours before set them up for the analysis, this procedure was carried out in all the samples to avoid any humidity interfere on the analysis.

Crystalline phases present in the sample

The crystalline phases in both samples were identified by X-ray diffraction analysis, XRD scans were obtained using a Bruker D8-A25 powder diffractometer with Cu Kα (λ =1.5406 Å for Kα1 and λ =1.5445 Å for Kα2, I1/I2= 1.89) 40 kV and 40 mA, a Ni chromator to filter out Cu Kb radiation, and a Lynxeye (PSD) detector. The scans were performed between 5°2θ and 55°2θ with a 0.019° step size and a counting time of 0.8 s per step. The qualitative identification of all phases was performed with Bruker Diffracc.EVA v4.2.1 software using the PDF-2 and COD databases.

Firstly, the crystalline phases of both materials were determined using the software mentioned before. Afterwards, five samples from the two materials were collected, two of them were used to identify the content of amorphous phases in each C&DW samples (FC and FM), for this purpose alumina was used as an external pattern (Pattern used = 25 wt%) in a vial with a total content of 3 grams of a blend between de sample and the pattern. Once the results were available, the Eq. 1 was used to obtain the percentage of amorphous phase:

$$Amorphous\ phase\,(AP\,\%) = \frac{Pattern\ \ XRD\,(\%) - Pattern\ \ used\,(\%)}{Patern\ \ used\,(\%)} \quad (1)$$

The other 3 were obtained from three different stages during the calcination of the FMG sample until 900 °C. One of them was treated up to 400°C, the second one up to 450 °C and the last one was thermally treated until 900°C, all of them were analysed with XRD to observe the phases formed during the process.

Scanning electron microscopy

Scanning electron microscopy (SEM) was performed using a Hitachi TM-1000 table–top scanning electron microscopy equipped with an energy dispersive X-ray spectrometer (EDS). images and qualitative chemical analyses of the samples and the cement mix obtain in the reactivity test were obtained

Plasticity

The plasticity index was calculated through the Atterberg limit test, being the inferior limit the plastic limit (PL) and the superior the liquid limit (LL). These two values are obtained with the next methods:

1. PL: In this test, a soil sample is gradually rolled into a thread and the point at which the thread breaks is noted by cracking up in two spots once it holds. The test is performed using a device called a "rolling device" or "plastic limit apparatus."

2. LL: In this test, a soil sample is taken and placed in a cup. A groove is made in the soil with a standard tool called a "liquid limit device," and the number of blows required to close the groove is determined. The test is repeated several times with varying amounts of water until the number of blows required to close the groove falls within a specific range. This range is known as the soil's liquid limit. Once the data has been collected, the regression line is set and the percentage of water obtained by replacing the number of blows equal to 25 in the equation, will be the superior limit.

Thermal behaviour

Thermal analyses of samples were obtained by simultaneous differential thermal analysis and thermogravimetry (DTA–TG), using a TASCH 414/3 model (Netzsch, Selb, Germany). Analyses were carried out in the temperature range 25–1200 ◦C and 25–900 ◦C, depending of the analysis, under air atmosphere, at a constant flow rate of 80 mL/min, in an alumina (Al2O3) crucible and at a heating rate of 5 ◦C/min. The amount of pattern used was ~80 mg.

Each analysis was performed three times with a different sample amount, carried out with a sample content below, over and similar to the pattern's weight, choosing the best graph adjusted to the baseline as the representative graph used for the analysis. The first analysis was carried out in all four samples (FC, FCG, FM and FMG) until 1200 ◦C to observe the general thermal behaviour of them, afterwards a maximum treatment temperature was defined on 900 ◦C.

Pozzolanic reactivity using R^3 bound water (BW) test

The R^3 test (Avet et al, 2020) is based on the idea of fulfil the conditions to simulate the setting and curing of a mix after 28 days, in a shorter period of time (8 days) and determining the chemical reactivity of the samples through the value of the Bound water (BW) using the Eq. 2:

$$Bound\ water = \frac{Wo - Wt}{Wo - Wc} * 100 \qquad (2)$$

Where, **Wo** is the weight obtained after the first drying and cooling of the sample of 10 grams, **Wt** is the weight of the sample obtained after the thermal treatment up to 350ºC from 5 grams of the sample previously dried and **Wc** is the weight of the container used for the sample. The procedure was followed as described in Figure 2.

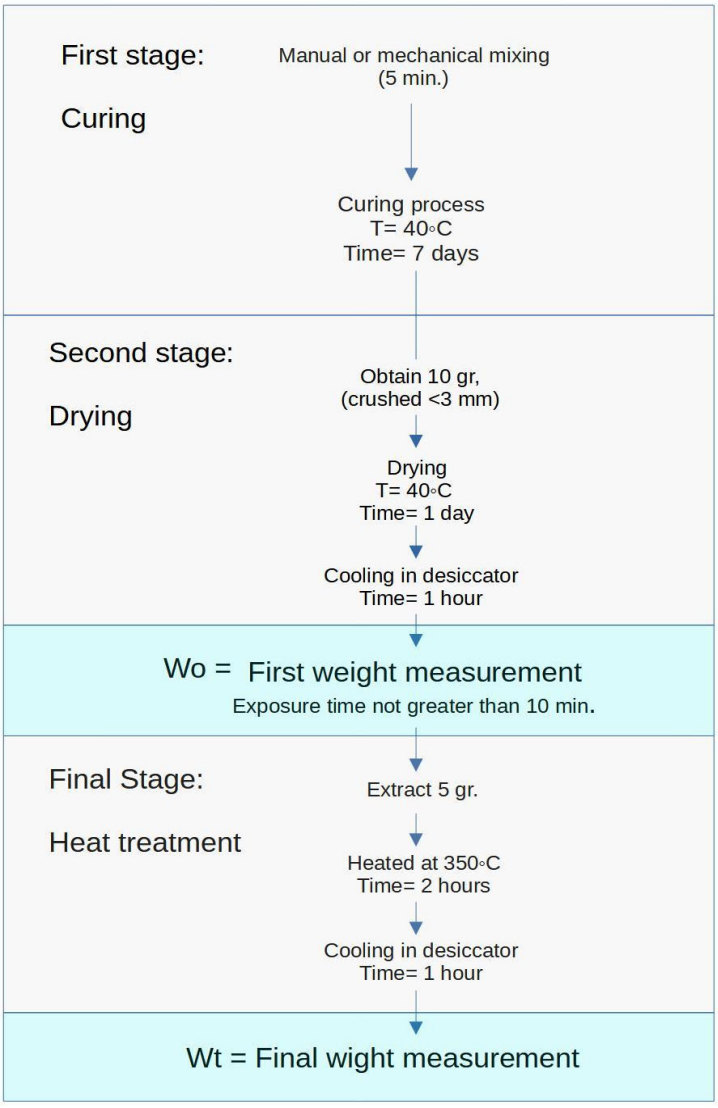

Figure 2. Process diagram to determine bound water using the description made by Avet et al, 2020.

Table 1. Materials used and their content in the mix (gr).

Raw material Content	SCM	Ca(OH)2	Deionized water	KOH	K2SO4	CaCO3
Sample	11,11	33,33	60	0,24	1,2	5,56

Once the BW was determined, as there is no apparent threshold that describes a low, medium or high pozzolanic reaction that we could use to present a proper conclusion, the compressive strength/BW relation described in "Comparison of the effects that supplementary cementitious materials replacement levels have on cementitious paste properties" (Ramanathan et al, 2020) was used to obtain a comparative parameter. The linear regression shown in this article (Eq. 3) has an acceptable R^2= 0,86, so it was used to calculate the compressive strength in function of the BW obtained in the experiment.

$$Compressive\ strength = 5{,}49 * BW - 21{,}09 \qquad (3)$$

Results and discussion

The chemical composition obtained by the XRF analysis, showed that All the samples have similar chemical composition. Despite the FC sample was obtained from a different area as the FM sample, both samples has similar chemical composition and their differences relay on the raw material that composed them, as the FC sample come from pure concrete fine aggregate waste, it has more calcium, instead the FM sample has a mixture between concrete waste, bricks and ceramics with other inorganic compounds, that means that is potentially made of mostly low grade clays, feldspars, micas and other soil minerals with higher content of quartz and aluminium. In this way, as both samples have similar chemical composition with lighter variations as it is shown in the Table 2, if the mineralogic analysis manifest similar mineral in some of the silicate content, would be accurate to say that the source of the raw material that forms them were produced from the same geological stratum.

Table 2. Chemical composition of the 5 samples by XRF.

XRF (content in %)			
Chemical composition	FC	CW	FM
SiO_2	21.15	19.99	28.26
TiO_2	0.37	0.47	0.57
Al_2O_3	5.30	6.88	9.43
Fe_2O_3	3.25	3.72	4.84
MgO	1.65	2.41	2.55
CaO	39.77	37.35	23.39
K_2O	1.10	1.56	2.08
Na_2O	0.00	1.49	0.00
SO_3	2.98	1.42	2.43

The crystalline phases obtained by the XRD analysis (Table 3) corroborate the observation made in the beginning, as the content of calcite is higher in the FC sample than the FM due the higher presence of calcium carbonate due the concrete that conforms it.

Table 3. Crystal and amorphous phases (calculate with the external pattern added) determined by XRD analysis, in wt%.

Phases	Class/Group	FCG	FMG
Calcite	Carbonate	18,88	13,97
Dolomite	Carbonate	2,56	0,00
Kaolinite	Phyllosilicate/kaolinite group	0,00	5,37
Dickite	Phyllosilicate/kaolinite group	2,56	2,15
Biotite	Phyllosilicate/mica	0,00	5,37
Gypsum	Sulphate	0,00	3,22
K-Feldspar	Tectosilicate	24,71	8,60
Albite	Tectosilicate	0,00	8,60
Quartz	Tectosilicate	35,49	23,64
Rutile	Oxide	0,85	1,07
Amorphous phase	Amorphous	14,80	28,00

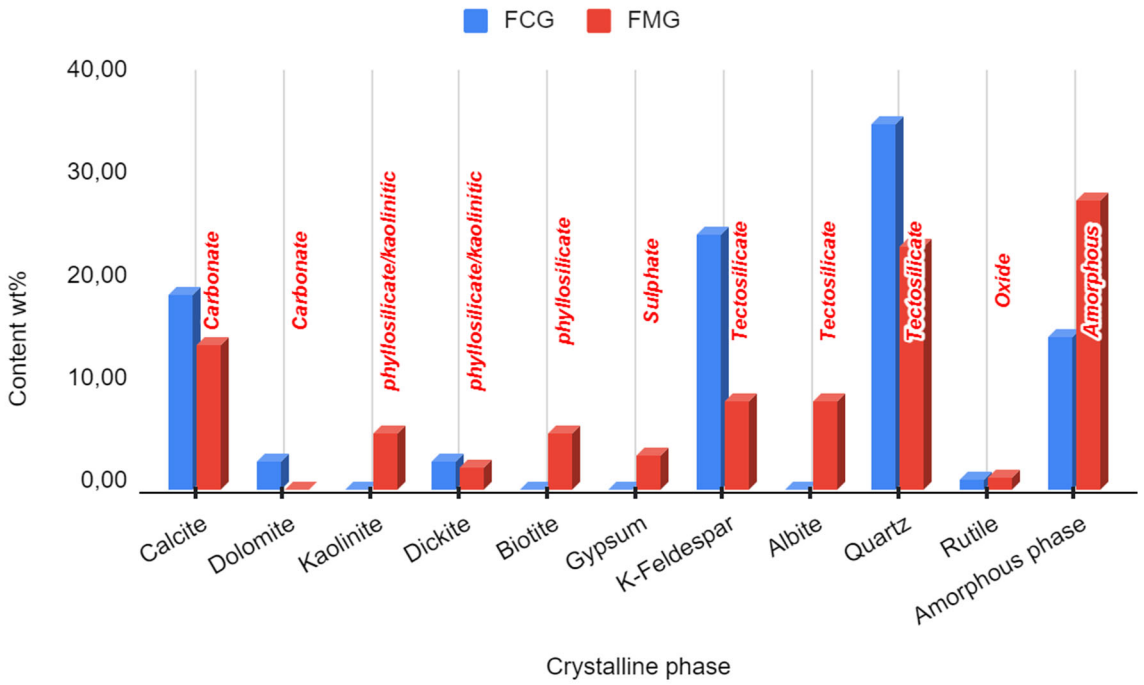

Figure 3. Graph of the phases present in both materials obtained by the XRD analysis.

The carbonate and tectosilicate minerals are the major components of the crystalline phase, representing the 21% and 60% of the total weight respectively for the FC sample, and the 14% and 41% of the total weight respectively for the FM sample. The FC sample has approximately a 50% more of relative weight of calcite and minerals from the tectosilicate group than the FM (53,4% more minerals from the carbonate group and 47,4% more minerals from the tectosilicate group), being the most abundant phase in this last group the quartz content for both samples. This variability is probably associated to the amount of soil, brick and ceramic waste that has been mixed with the concrete in the mix fine aggregate waste. This two major groups plus the amorphous phase account the 96% and 82% of the total weight for the FC and FM samples respectively as it is shown in the Table 4. It is worth to note that the calcium aluminate hydrates gel (CAH), responsible of the strength gain rate in early ages , it is an hydraulic crystalline phase formed during the hydration of the cement paste that is connected with the compressive strength achieved by the calcium aluminate cements pastes (CAC), and it depends highly on the content of alumina in the amorphous phase that can form the amorphous AH_3 gel that react with the Ca+2 forming crystalline phases as C_2H_8 and CAH_{10} among others. The unreacted fraction could act as a filler around the crystal skeleton (Ding et al, 2020), even this two phases can undergo a phase transition to C3AH8 (Alite), also Afm phases can be form using as a catalyzer nitrate, in expense of C_2H_8 and CAH_{10} crystalline phases formation(Falzone et al 2015). But normally this reaction occurred in the presence of calcite, ettringite and/or gypsum, once the gypsum on the solution is fully depleted by the monocalcium aluminate (forming ettringite and

amorphous AH_3), and in the presence of residual monocalcium aluminate phase, this last compound react more favourable with calcite to form hemicarbonaluminates and monocarbon aluminates crystalline phases rather than react with the ettringite to form monosulfoaluminate (Julien Bizzozzero, et al,2015). This last process also could be trigger by the presence of tricalcium aluminate (Chaipanich, et al, 2020) .

The higher content of amorphous phase in the FMG sample is due to calcined clays, as they are the ones that are present in bricks or any ceramic used in construction, that have a major content of amorphous phase (SKibsted et al, 2019). Also, one particular observation can be made by the amount of calcium oxide in the carbonate group respect to the amorphous phase (Amp) represent a fraction of 1,15 (CaO/Amp) for the FCG sample and 0.48 for the FMG, that could give potential information for the determination of amorphous phases from the CaO content until a certain threshold.

Table 4. Minelogical composition of FCG and FMG determined by XRD analysis, in wt%.

Group	Minerals	FCG	FMG
Amorphous	Amorphous phase	14,8	28,0
Tectosilicate	Albite	0,0	8,6
Tectosilicate	K-Feldspar	24,7	8,6
Tectosilicate	Quartz	35,5	23,6
Total Tectosilicate		60,2	40,8
Carbonate	Calcite	18,9	14,0
Carbonate	Dolomite	2,6	0,0
Total Carbonate		21,4	14,0
Total		**96,4**	**82,8**

On the other hand, as was expected, the amount of kaolinitic clays in the FM sample is superior in almost twice in content, but it represents just 7.52 % of the total weight of minerals in the FMG sample, being kaolinite the major phase. Dickite, the other clay mineral of the kaolinite group that is present in both samples, is one of the minor phases which, alongside the Rutile (Oxide group) , are the only minor crystalline phases in which the FC sample is formed.

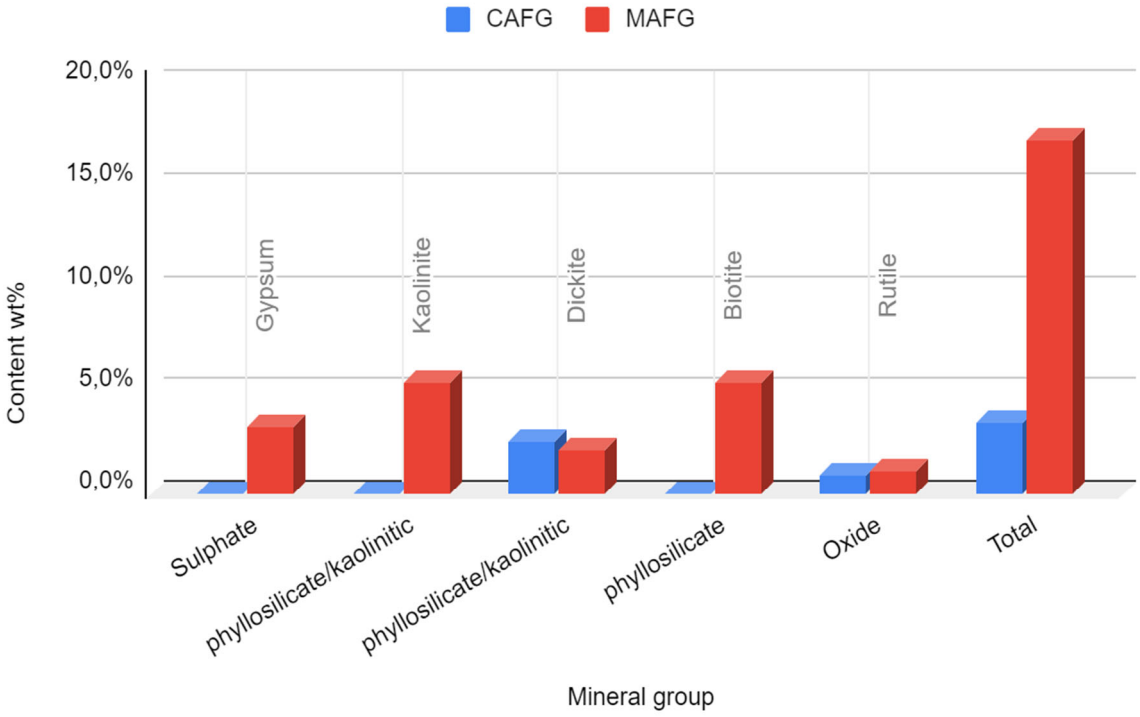

Figure 4. Minor crystalline phases in FCG and FMG samples.

The plasticity test indicates that the materials has low plasticity, and there is a big difference between the plasticity of the concrete waste and the concrete fine aggregate waste, that could be due the mineralogic characteristics of the waste material (this weren't analysed) as it could be mixed with some low clay minerals from soil that could have given it some better plasticity, or rather it could have been due the flocculant used in the FC sample during the sedimentation, that reduced the plasticity of the sample.

In the Figure 5 it is possible to distinguish the fact mentioned before. Also, the FM sample has the best index due the clear larger amount of clays in its structure in comparison to the FC sample. It's peculiar, that once the samples were treated mechanically the value of the index decreased for both materials, and ended up both with almost similar values, parameter that was not deepened in this research but will be important to clarify. This differences among the plasticity index might be significant in the analysis of workability of the materials, which wasn't part of the scope of the present research.

Table 5: plasticity index plus range of plasticity (lower and upper limits), in wt%.

Results	IP	Lower limit	upper limit
ARMH	7,79	43,18	50,98
ARMH_R	4,00	37,98	41,98
FC	5,65	48,03	53,68
FCG	3,68	37,15	40,83
CW	7,22	30,45	37,68

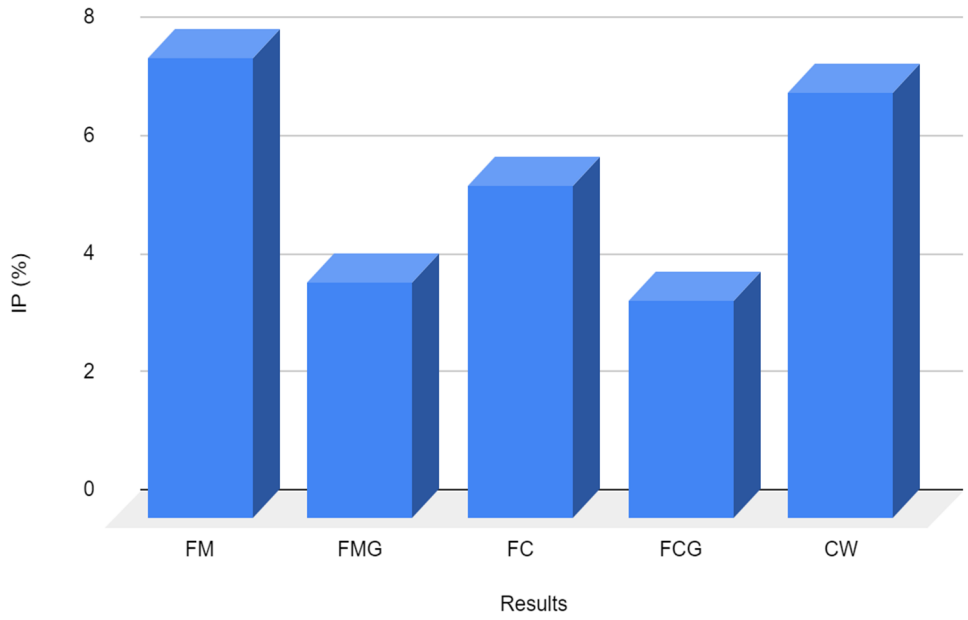

Figure 5. Materials and its plasticity index.

In the granulometric analysis, it has been observed that the flocculant might have affected this analysis due the interaction between the pyrophosphate and the additive used in the sedimentation of the fine particle aggregate waste, to confirm this statement the next procedure was followed.

The first results of the size of the particle without any mechanical treatment were obtained. This showed that the size particle of 90 percent of the total volume of the FC and FM samples were 78.33 µm and 51.63 µm respectively. On the other side, once the samples were grinded by the ball mill, the graph showed a histogram that did not follow normality on its distribution, showing also a diameter of particle of 90 percent of the total volume of 376.9 µm for FCG and 126.5 µm for FMG (Figure 7). These results weren't representative and gave light that something was offset on the analysis, giving the idea that the flocculant could act as an organic resin that binds some of the grains due the mechanical pressure exerted by the iron balls. Inhibiting the size particle reduction or, as

simply as that this flocculant interfered the analysis of laser granulometry, inhibiting the function of the pyrophosphate as separator between the grains within the samples. Due this, a second experiment was carried out, using this time a disc mill set in two minutes for all the samples, repeating this process in both samples and adding another one made of raw concrete waste, without any additive or flocculant (CWG). This repetition allows us to confirm that the last results were reliable, as the graphics and size particle distribution showed the same outcome. Also, it was backed up by the results given by the CW sample, that showed a graphic with a better size particle distribution with a mean of 11.42 μm with a 90 percent of volume of particle's diameter of 36.51 μm (Figure 8). Showing some irregular size distribution at the upper threshold associated with the bigger size particles, probably due to a minor grade of some organic waste content that is possible to find in this kind of residues (Marlunk E. et al, 2018) or/and the amount of quartz and clay like minerals present in the soil. The FC will show higher volume of particles with bigger diameter and FM will show a bigger volume of particles of smaller diameter. The latter, due the different hardness index between the clay like crystals and the quartz, as can be observed in another article recently published (Wu Huixia et al, 2023). Then, the content on quartz and clays in soils will determined the particle distribution achieved by the grinding work of the mechanical reduction.

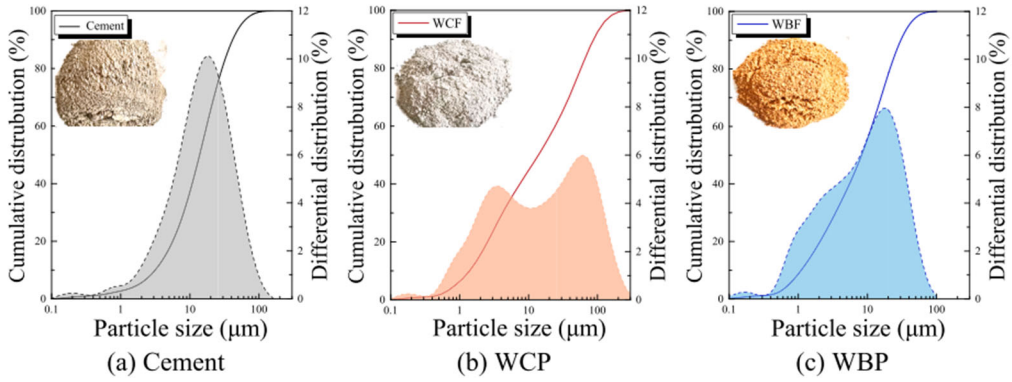

Figure 6. Different size particle distribution for a) Portland cement b) Concrete waste c) Brick waste (Wu et al, 2023).

To prove the assumption that the flocculant is affecting the analysis, the sample obtained from the second reduction was analysed using three sieves of 150 μm, 100 μm and 63 μm. The results showed that the size of the grain below 63 μm corresponded to 95% of the total volume, demonstrating that the reduction of the grain size wasn't entirely disrupted by the flocculant used but it has a clear consequence on the detection of the grain size by laser granulometry (Table 6). Also, it is possible to see clear differences between the DTA/TG of the first material and the milled one (as will be exposed further), specially attributed to the different timings of the thermodynamics associated by the decarbonation process, which is a consequence of the flocculant rather than the size particle reduction.

Table 6. Comparison between the results from sieving and the laser granulometric analysis.

Size particle (SP µm)	Sieving sample (gr.)	Content Sieve (%)	Laser granulometric analysis (%)
SP < 63	908,793	95,35	50,10
SP [63, 100]	37,561	3,94	12,85
SP [100,150]	6,175	0,65	25,77
SP >150	0,593	0,06	10,00

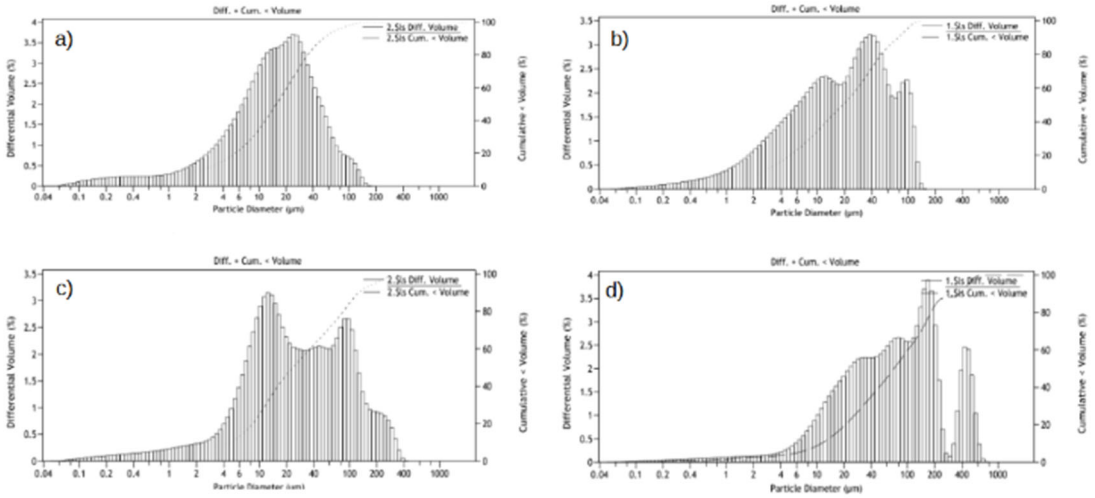

Figure 7. Particle size Distribution of the C&DW before grinding a) FM sample b) FC and after grinding c)FMG Sample d) FCG Sample

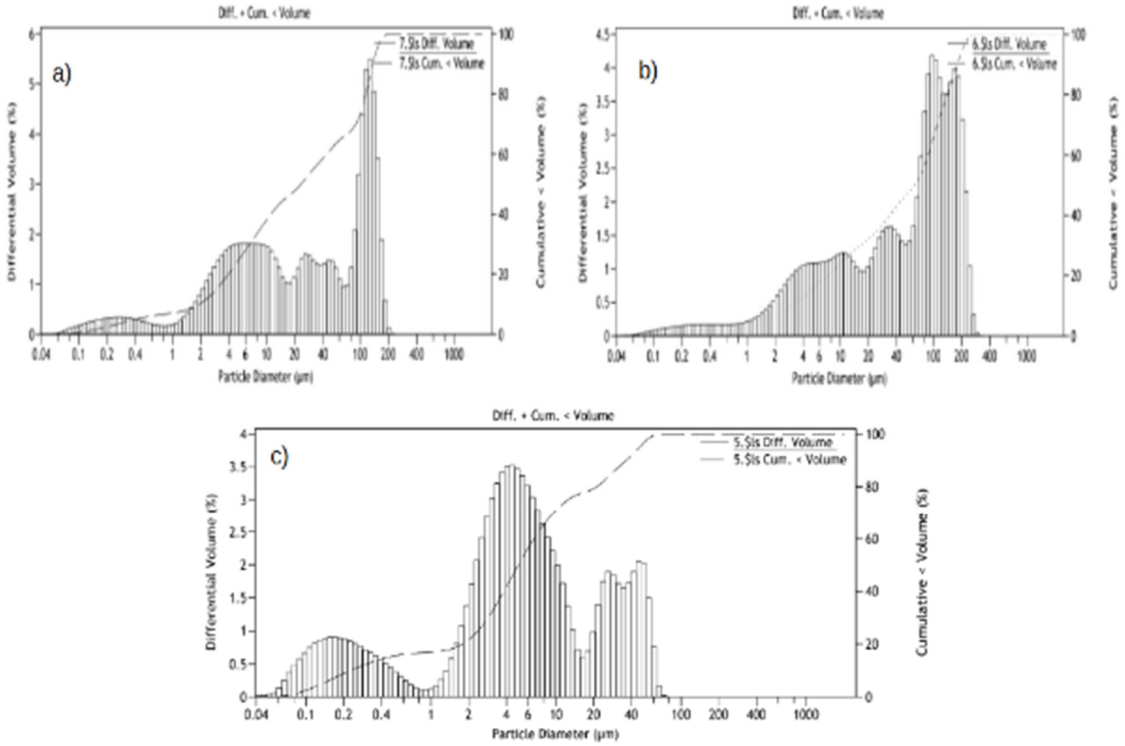

Figure 8. Particle size distribution obtained after grinding a) Sample FMG b) Sample FCG c) CWR

Beside this result, the thermal behaviour of all these materials showed a particular tendency to displace to slighter lower temperature the endothermic decarbonation peak that occurs around 800 ◦C once it is grinded. In the beginning was taught that this behaviour was due the reduction of the particle size, but was evident after the results of the DTA obtained from the CWG sample, that this phenomenon is not attributed to the particle size reduction but due the organic compound used in the sedimentation recycling process, as this displacement did not occur on this material. Being the flocculant the architect of the condition that would allow this to happen, particularly during the first half of the calcination (up to 450°C), as any additive or organic compound is decomposed before 450°C (Moropoulou et al, 1995). Accelerating the reactions that involves the consumption of the calcium carbonates to lower temperatures as it is shown in Figure 9. Also, the difference in between the maximum peak of decomposition of CO_2 among the samples with different mineral composition, is due the kind of carbonates minerals that form the material, as the FC has some dolomite in its mineral composition the peak of it before the grinding is close to the 870 °C, instead, the peak of the FM sample that has just calcite on its composition, is below the 850 °C, which is correlated with the literature (Moropoulou et al, 1995).

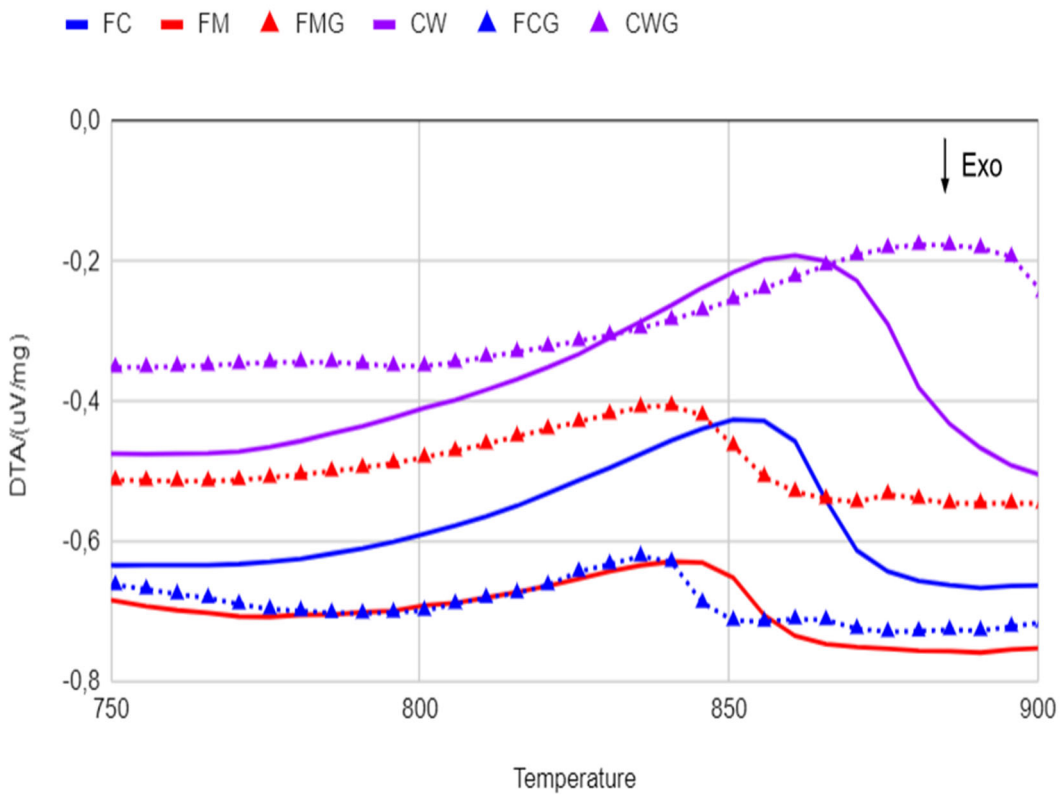

Figure 9. DTA of all samples at a temperature treatment close to the decarbonation peak.

From all the samples, the FMG was chosen to assess the crystalline phases formed after the calcination of the material up to 900°C for two hours due its minor amount of carbon dioxide produces during the calcination process, value that was corroborated with the stoichiometric analysis carbon dioxide content from the carbonate minerals (calcite and dolomite). From the XRD analysis the Table 7 has been created.

Table 7: Mineral composition of FMR and FMRC sample obtain from XRD, in wt.%.

Class/ group	Minerals	FMR	FMRC
Tectosilicate	Albite	12	9
Tectosilicate	K-Feldspar	12	12
Tectosilicate	Quartz	33	26
Sulphate	Barite	0	2
Sulphate	Gypsum	4	0
Sorosilicate	Anhydrite	0	8
Sorosilicate	Gehlenite	0	10
Phyllosilicate/kaolinite	Dickite	3	0
Phyllosilicate/kaolinite	Kaolinite	7	0
Phyllosilicate/Mica	Biotite	7	0
Oxide	Rutile	1	0
Inosilicate	Diopside	0	8
Inosilicate	Larnite	0	11
Inosilicate	wollastonite 1A	0	13
Carbonate	Calcite	19	0

The FMG sample will be used to make a rehydrated cement from a thermally treated mix made of recycled concrete and calcined clay minerals (bricks and ceramics). Then, it is expected that the mix behaves as the two components named before. Taking this in account, it is well known that during the thermal treatment of these raw materials certain processes of activation, decomposition and recrystallization can be observed for each group individually. Firstly, as Angulo mentioned in their research (Angulo. et al, 2022), for the rehydrated cements fabricated with thermally treated recycled Portland cement, between 50°C and 250°C, calcium sulfoaluminate as ettringite and sulphates as gypsum are decomposed. In this case gypsum decomposes completely forming Anhydrite and barite. It is important to mention that some of the sulphur is latent in the amorphous phase presenting unidentified structure due its grade of disorder, then it cannot be detected by XRD analysis. So, the use of an external pattern was necessary to quantify this value, even so it is needed to note that due the semi quantitative characteristics of the Rietveld method, the exact amount of sulphur in amorphous state is not possible to determined, but it is probable that this amorphous phase would have crystalized during the calcination process forming the extra anhydrite found in the material and the small amount of barite, both minerals were detected by SEM analysis (Figure 10 and Figure 11).

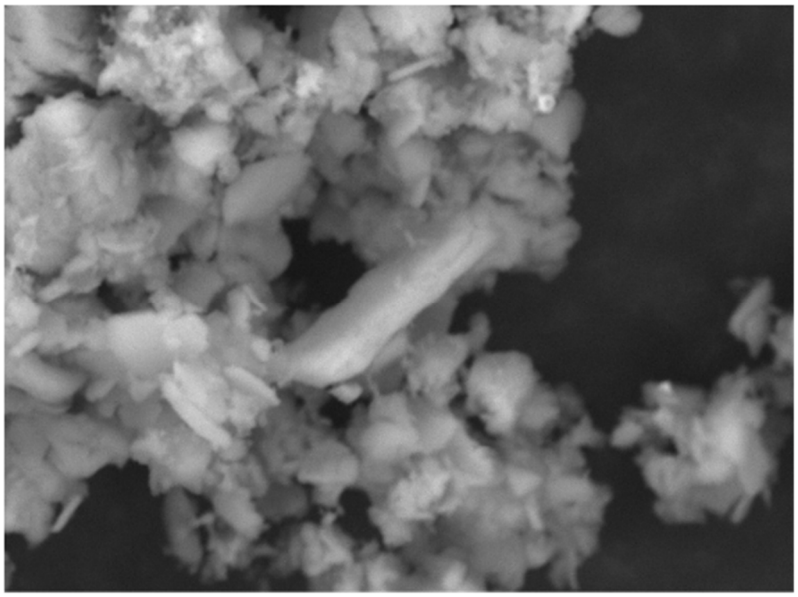

Figure 10. SEM image of the C&DW treated bat 900 °C. Anhydrite at the centre of the image.

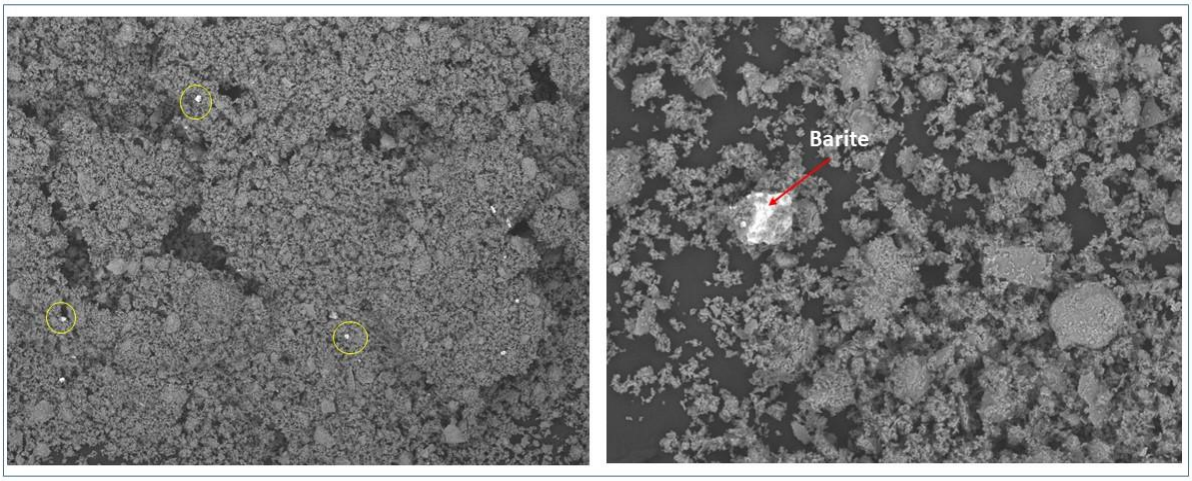

Figure 11. SEM image of the C&DW treated bat 900 °C. Left: general view, with white dots representing the barite. Right: Barite Crystal.

The DTA/TG analysis shows an endothermal hump can be observed between the 324°C and 450°C (using the first derivative as reference) that could be due the exothermic reaction that can produce an organic additive, normally used to promote carbonation and improve workability, settling time and durability, within the range of 300-500°C (Moropoulou et al, 1995) (Figure 12). Also the C-S-H hydraulic phase that dehydrated from the 100°C to the 650°C, forms mostly amorphous phase that is relevant for the strength gain of the recycled cement pastes (Angulo et al, 2022) but in this case, just the albite could be responsible for some CSH gel into the amorphous phase and trigger some recrystallizations but probably most of the inosilicates formed after the 450°C (samples at this stage were taken and did not showed any transformation by the XRD analysis), coming from reactive phases that were in the amorphous content.

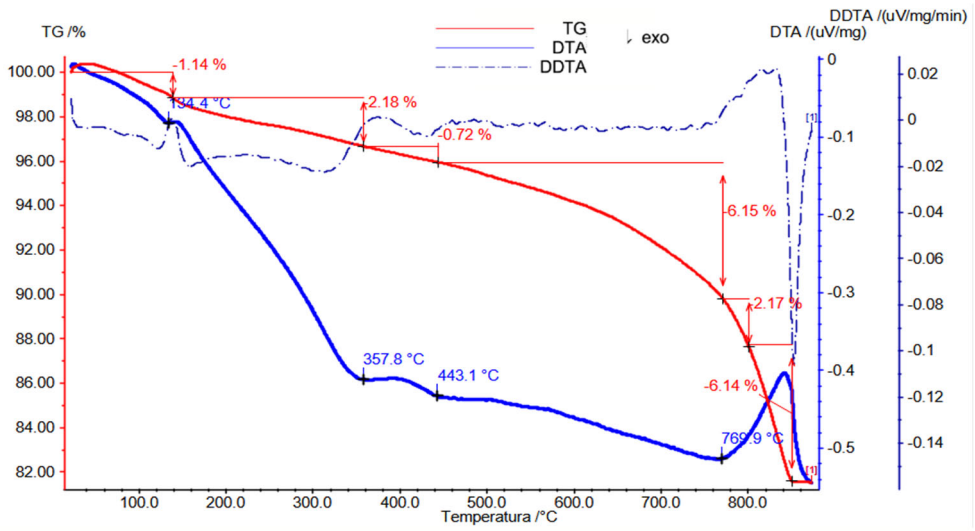

Figure 12. DTA/TG of FMR calcined up to 900 ◦ C

Observing the results of the Figure 7 it is possible to detect three main endothermic peaks, one by 134°C, the second one between 358-443°C and the peak by 800°C, this last one is related with the decomposition of CO2 from the carbonates. This peak of mass loss was compared with the stoichiometric value taken from the content of carbonates on the sample before calcined, which was similar with the mass loss given by the DTA. But on the other hand, once these values were compared in the FCG sample, there was a difference of approximately 3%. This result was analysed using the DTA/TG curves, contrasting the values given by the FCG, FMG and CWG sample (Figure 13).

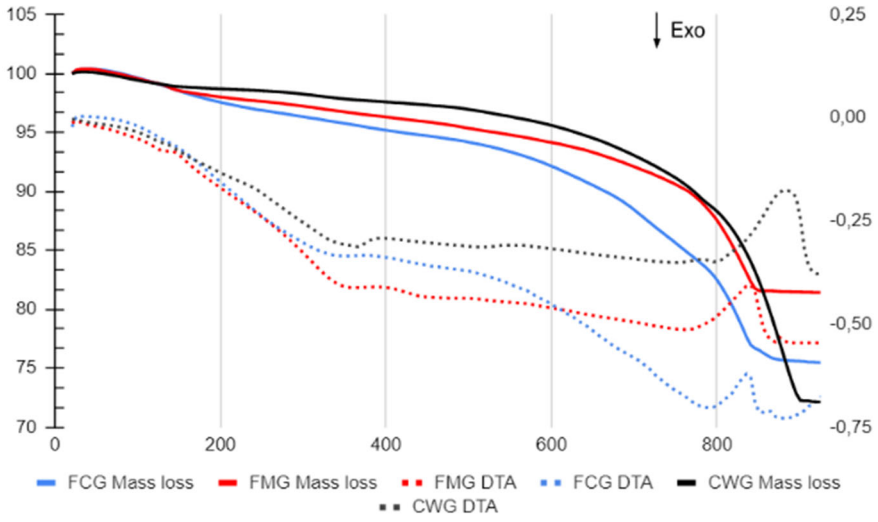

Figure 13. DTA/TG contrast between FCG, FMG and CWG samples.

These results show that although the FCM has a higher amount of carbonates, it presents a similar mass loss than the FMG around 800°C and a difference of around 3% from the stoichiometric values of carbon dioxide due its carbonate content has been calculated. Observing that FCM has roughly 8% major mass loss in between the 500 and 780 in comparison to the FMG sample. This can be explained, as the decarbonation reaction starts in an earlier stage, as carbon dioxides starts to be released from 600°C onward (Moropoulou et al, 1995), where the maximum peak is around 800°C. Then this phenomenon can be explained taking this into account. So, 3% of this weight loss could have been due the early decarbonation of the calcite and/or dolomite in the sample. As the mass loss due decarbonation given by the DTA/TG is around 6.54% (Annex 3), there is 5% of this mass loss that is hard to identify how it is produced. Mainly because a small amount of Dickite cannot explain the whole loss, noting that it is understood that this mineral is decomposed during the calcination, adding into the system sulphur that can be used in further crystallisations. Then some reactions related with the amorphous phase might be the cause of these differences.

Technically the FMG sample should have a higher reactivity by that temperature range due the major amount of soil with clays on it, meaning that the mass loss would be higher for FMG sample at this stage, which is clarified when we compared the mass loss between the FMG and CWG, as can be seen in Figure 13. Then if we assume that due to the similar chemical composition in between the FCG and CWG, the mineralogical compositions also would be similar as they share the same geological origin. Then it is very probable that the flocculant used in the process of sedimentation, is reacting with all forms of water content (H_2O and OH^-) existing in the amorphous phase of this sample and making possible this difference in the mass loss. If the mineralogic composition is different, then more research is needed to clarify this point.

In this way, to determine the carbon dioxide emitted during the calcination process of the recycling materials. And assuming the full decarbonation of the carbonates for the FCG sample once it's calcined. The stoichiometric volume of carbon dioxide calculated from the carbonates in both samples, will be used to calculate the amount of carbon dioxide emitted by the materials once they are thermally treated (Table 8 and Table 9).

Table 8. Relative CO_2 produced by both materials, in wt%.

Mineral	CO_2
Calcite	43,97
Dolomite	47,73

Table 9. CO_2 produced by both materials during calcination using stoichiometric analysis, in wt%.

Sample	FCG	FMG
Calcite content	19,00	14,00
Dolomite content	3,00	0,00
CO_2 Calcite	8,35	6,16
CO_2 Dolomite	1,43	0,00
Total CO_2 (%)	9,79	6,16

Second and last, the ceramic and clay materials have different thermal behaviour. As the content of clay is purely from the kaolinitic group, being the kaolin the most abundant phase, followed by dickite. Then it is well known that all the kaolinite minerals go through a process of dihydroxylation where the hydroxyl groups are moved from the interlayer structure making them collapse and form a metastable kaolin, which is a highly reactive amorphous phase. All these reactions occur between 500-900°C (Skibsted et al, 2019). These resolutions are consistent with the mineralogic results obtained in the XRD of the calcined sample, where the kaolin and dickite formed reactive amorphous phases, as there are no signs of these crystals on this sample.

There have been researches around the dynamics of the C-S-H chains during the dihydroxylation that occurs above the 500°C, the results have shown that the structure of the gel collapse forming amorphous phases, and in other cases more favourable Ca-O-Si crystal phases (Yang et al, 2021; Zhang et al, 2019), in this way, it is possible to explain how the wollastonite, Larnite and Gehlenite are form. Also, in Yang´s article is mentioned that due the change of the weaker Ca-OH bond of the C-S-H gel to a more stable Ca-O-Si bond, It increased the stiffness and toughness of the system.

In another article, a triaxial cementitious material with a system of High Ca/Low Al (Portland cement, SCM and Limestone) were fabricated. This paste was further thermally treated. The sample obtained has similar ratio of Aluminium oxide than the FM, and it also forms crystals of Gehlenite, Larnite and wollastonite. It is also mentioned that the CaO/SiO_2 ratio is related with the preference formations among these phases, agreeing that with ratios close to 0.28, Wollastonite and Gehlenite formation were favoured over larnite (Donatello et al, 2013). In this research, CaO/SiO_2 = 0,8, favouring the formation of wollastonite but instead of major content of gehlenite over larnite, it has as slighter more content of larnite. This value could be associated to an instrumental error, and we can assume that at this rate, the value of Gehlenite and Larnite are equals. The wollanstonite was identified by the SEM-EDS (Figure 14)

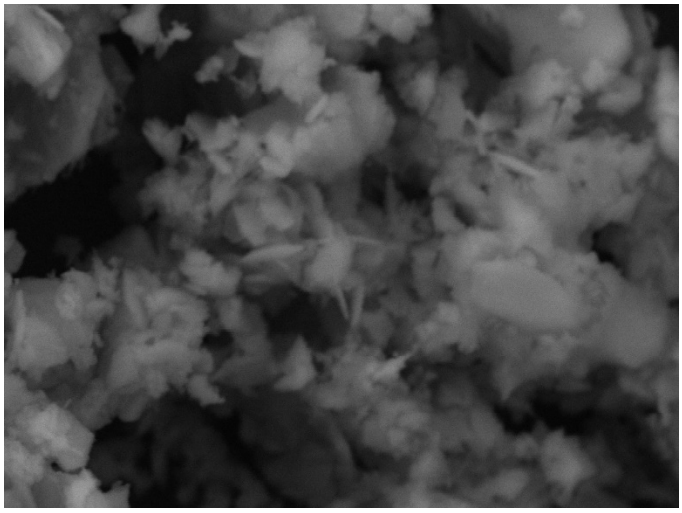

Figure 14. SEM image of the C&DW treated bat 900 °C. The needle-like textures are wollastonite crystals.

The reactivity test of the C&DW provided result exposed in Table 10.

Table 10. Reactivity test (R^3): bound water and compressive strength.

Sample	Water bound (g/100g)	Compressive strength (MPa)
Metakaolin	8,953	28,062
FCG	8,964	28,122
FCNP	9,079	28,756
FM	8,978	28,202
FMG	8,992	28,275

These results show that despite knowing that the metakaolin has high pozzolanic activity, this sample showed the lowest water bound among the materials tested, being the raw concrete paste without any treatment, the one that obtained the highest value of bound water. This backed up the idea of the flocculant as an influential agent on the physicochemical reaction that occurred during the thermal treatment, which also affects the hydration of the triaxial cementitious paste used in the experiment (PC, SCM and calcite). This statement is visible due to the differences between the FCNP and the FCG sample. Although the values are relatively close one each other and even if the flocculant could have affected the bound water values, these results did not present a significant difference with the rest of the samples, which could make this fact instead of a problematic, an opportunity to improve the speed of the reactions during the thermal treatment with a low decline of mechanical properties. Wider studies related to the consequences of keeping up the organic compound have to be assessed before taking a decision about keeping this organic flocculant in the recycling process, as it has been seen that this additive modifies greatly the behaviour of the material with pure fine concrete aggregate

waste that could bring a different outcome related with the development of the compressive strength in long term of the FCG sample.

Also, as the mineralogic composition of FCG sample once it is calcined at 900°C was not analysed. The DTA analysis in between all samples shows some similarities related with the thermodynamics of the materials once they are calcined, showing differences in the size of the endothermic and exothermic peaks. As it is possible to observe in Figure 15, the curve of the DTA of CWG is the only one that has an endothermic peak around the 790°C just before the decarbonation endothermic reaction. The rest of the samples have high activity between 500°C and 800°C but neither of them have any particularly strong and defined peak. But, considering the analysis made in between the FCG and FMG samples, and taking in account the influence of the organic additive in the reactivity of the FCG sample. Then it is possible to confirm that the materials used in constructions all around the Barcelona area, have similar mineral composition and would react very identically once they are thermally treated if flocculant is not used. The composition of the mix material will vary just due to the amount of ceramics content; thus, it will affect the content of quartz, feldspars and clays. But at first sight these differences won't make significant variation on their mechanical properties.

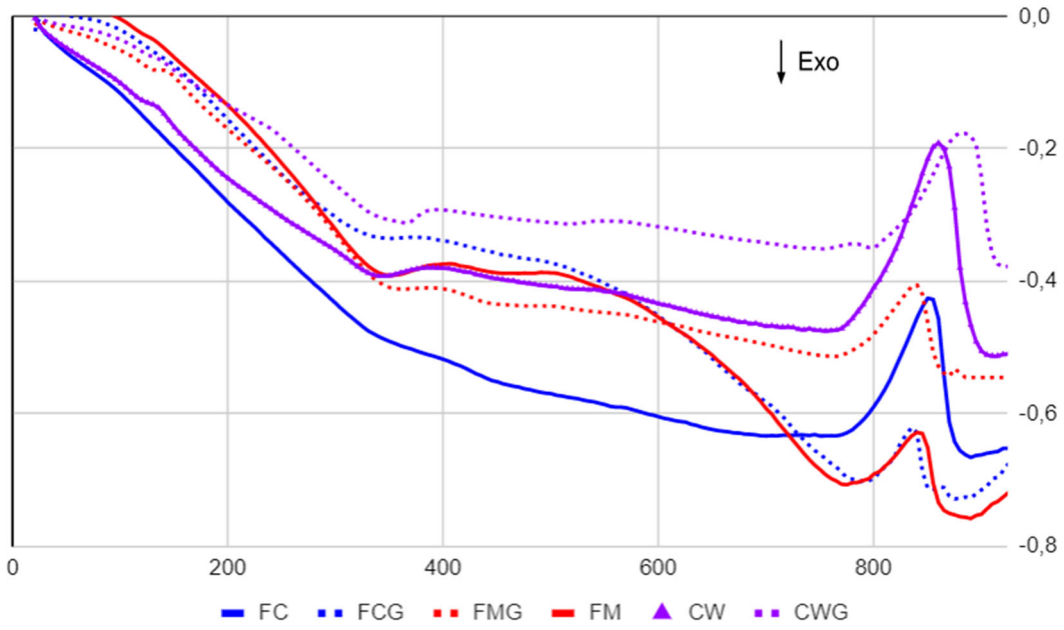

Figure 15. DTA of all samples.

Studies had confirmed what have been seen on this research, showing that demolition and construction fine aggregate powder obtain from recycling concrete has same pozzolanic reactivity than the one obtains from recycling clay (Liu et al, 2014), due this, the hybrid form of these two fine particle wastes can be used as partial replacement of Portland cement. The addition of calcite in the paste, beside of allowing the early reaction of carbon aluminate phases, it also reduces the buffer capacity of the paste (resistance to the pH change once a base or alkaline mineral are added), which it

might not affect negatively the corrosive effect of the atmosphere in the long term, cause the residual calcite act as filler reducing its porosity and permeability (T. Matches et al, 2007).

Finally, and to understand the impact of this sort of materials as substitute of the Portland cement, it is necessary to take in account that the production of Portland cement generate around 0,8 ton of CO_2 per ton of PC (Turner et al,2013) and considering that between 50-60 % of the emissions are from the calcination of the calcium carbonate as it is the main raw material in the clinker production (Benhelal et al, 2021). Then, it is possible to gather this information plus the data collected during this research, to determine the CO_2 reduction with the values of the CO_2 of the stoichiometric balance according to the mineralogic composition of carbonates in the sample. In this way, have a quick idea of the CO_2 reduction in view of a possible scenario where we have a partial substitution of Portland cement by SCM.

To calculate this is necessary to clarify that the only variation on the process will be the material used and the maximum temperatures needed for the calcination, the crushing, milling and cooling processes might stay the same, then this analysis does not consider all the variables needed to get an exact value of CO_2 reduction, but it consider the reduction of CO_2 due the less use of PC and the CO_2 generated by the calcination of the SCM's (FMG and FCG), giving an idea of the potential CO_2 reduction with the different substitution grade shown in the Table 11. For the calculations, was considered that 60% of the CO_2 is due the calcination of the calcite or as it is put in the Table 11, the raw material. And the 40% left, it is due the process of crushing, grinding, thermal treatment and cooling that involves the clinker production (Benhelal et al. 2011). The latter value is obtained from the product between the total CO_2 eq of PC and the wt (%) of the CO_2 emissions due the mechanical and thermal treatment applied during the fabrication of PC.

Table 11. Calculation of CO_2 eq of material

Sample	CO_2 eq total	CO_2 eq raw material	CO_2 eq process	CO_2 Emission
PC	0,8	0,480	0,32	
FCG	0,37	0,054	0,32	0,0903
FMG	0,36	0,038	0,32	0,0637

CO_2 Production							CO_2 reduction (Mt)			
Scenary	Substitution %	PC (Mt)	SCM (Mt)	CO_2 PC (Mt)	CO_2 FM (Mt)	CO_2 FC (Mt)	FMG	%	FCG	%
S100	100	0	3,4	0,000	1,218	1,272	1,502	55,2	1,448	53,2
S76	76	0,8	2,6	0,640	0,931	0,973	1,149	42,2	1,107	40,7
S60	60	1,36	2,04	1,088	0,731	0,763	0,901	33,1	0,869	31,9
S30	30	2,38	1,02	1,904	0,365	0,382	0,451	16,6	0,434	16,0
PC	0	3,4	0	2,720	0,000	0,000	0,000	0,0	0,000	0,0

So, in the hypothetical scenario where we could use the whole amount of fine particle waste (76% of replacement) instead of PC, the reduction of CO_2 would be around 1,1 Million of tons of CO_2. Even so, the most plausible scenario nowadays, is the partial substitution of 30% of PC with SCM, that will reduce the emissions in between of 451.000-434.000 tons of CO_2, beside it will bring the increment of the C&DW Valorization up to 76,6%.

Thus, in this way, we can conclude that we have three benefits of the partial replacement. Firstly, there is a reduction of the carbon footprint, secondly there is a Valorization of the fine particle allowing to reach the strategic objectives set by the General Program of prevention and management of resources and waste in Catalunya in 2020 (PRECAT20) and finally, it would be possible to reduce the use of natural resources as limestone in the production of Portland cement. Creating in this way a reduction triangle that brings an economical and environmental benefit (Figure 16).

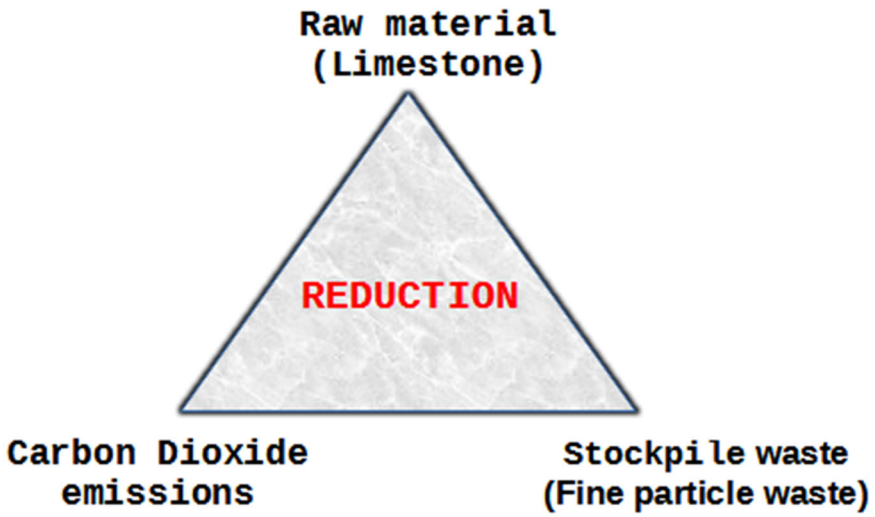

Figure 16. Reductions obtained due the use of SCM.

Conclusions

The characterization of the C&DW materials has shown that the wastes, although coming from different recycling plants, have similar chemical and mineral composition, as they all have a sedimentary origin from the Valles depression. The results obtained in the DTA/TG partially support this statement, as the exothermic and endothermic reactions observed in both materials have a similar behaviour. All of them presenting an endothermic peak by the 134°C due the loss of the tensile water, an exothermic peak by the 440°C due to organic additives, which in this case is highly probable that

this peak is related with the flocculant used on the recycling plant. And the last peak around the 800°C, related with the decarbonation of the carbonates, this last peak can start by the 600°C onwards, as it is the case of the FCG sample, probably influenced due the organic additive.

The mass loss differs due to three main reasons.

Firstly, the higher amount of clays from the soils, will lead a higher reactivity due to the higher amount of amorphous phase in the material. which produces a higher loss of hydroxyls due recrystallization processes between 500°C and 900°C. The amount of clays also affects the losses of bound water up to 200°C and hydraulic water, which is related to the mass loss between 200°C and 600°C in the DTA/TG analysis.

Secondly, the amount of bricks and ceramics in the mix will mean an inversely proportional content of calcium carbonate, the latter being the major cause of mass loss around 800°C when the materials are thermally treated up to 900°C. Being the FMG sample the one with the lowest emission of carbon dioxide, with a CO_2eq of 0,36 t of CO_2/t of concrete.

Thirdly, the additive used to settle the finest fraction of C&DW might affect some physicochemical reactions related to the dihydroxylation process that occurred in hydrated crystalline phases as C-A-S-H, CH, and C-S-H, but also in the amorphous phase of the material, once they are under thermal treatment. The activity of this hydrated phases in the amorphous phase are thermodynamically disrupted over the 500°C. This last reaction explains the bigger amount of mass loss in between 500°C and the beginning of the decarbonation endothermic reaction by 770°C for FCG sample, in comparison with the FMG sample. As due its low content of clays carried in soils, it should have had null o very low mass loss in this range of temperature. Phenomenon that did not happened due the activator function that the flocculant had shown on the materials. Accelerating and modifying some thermodynamic occurring during the thermal treatment.

The flocculant also has an influence in the analysis of the particle's size due its interaction with the pirophosphate, acting as an inhibitor of the particles separation.

Finally, it has been confirmed that the amorphous phase plays a fundamental role in the development of the mechanical properties of the cementitious paste made from recycled materials, and wastes, clean or not, they can have a high pozzolanic activity, even similar of the pastes made using kaolin. The material once calcined showed a considerable amount of wollastonite, Larnite and

gehlenite, formed by the crystallization of some of the C-S-H gel. At a rate of CaO/SiO_2=0.8, the formation of Wollanstonita is favoured over Gehlenite and Larnite, and this last two are formed in similar amount.

This will enable further study of the physicochemical reactions of the cement created with a partial replacement, using recycled fine C&DW as SCM. which will allow us to understand more accurately the thermodynamics that are involved in these processes and to quantify the influence of the organic additive on the reactivity of the paste.

References

Agència de Residus de Catalunya, 2021a. Informe 2021 de la declaració anual de residus industrials per a gestors (DARIG) http://estadistiques.arc.cat/ARC/estadistiques/Informe_DARIG_2021.pdf

Agència de Residus de Catalunya, 2021b. Balance estadistico 2021-Residuos de construccion y demolicion. PowerPoint Presentation (gencat.cat).

Andrew, R. M.Global \chem{CO_2} emissions from cement production, 1928-2018, 2019, Earth system science data, Vol. 11, no. 4 , pp. 1675-1710, DOI ,10.5194/essd-11-1675-2019, URL:https://essd.copernicus.org/articles/11/1675/2019/

Angulo, Sergio C. and Guilge, Mario S. and Quarcioni, Valdecir A. And Cincotto, Maria A. and Nobre, Thiago R. S. and Poellmann, Herbert, The role of calcium silicates and quicklime on the reactivity of rehydrated cements, Construction and building materials (2022) , Vol. 340, DOI 10.1016/j.conbuildmat.2022.127625

Avet, F., Li, X., Ben Haha, M., Bernal, S. A., Bishnoi, S, Cizer, O., Cyr, M., Dolenec, S., Durdzinski, P., Haufe, J., Hooton, D., Juenger, M. C. G., Kamali-Bernard, S., Londono-Zuluaga, D., Marsh, A. T. M., Marroccoli, M., Mrak, M., Parashar, A., Patapy, C., Pedersen, M., Provis, J. L., Sabio, S., Schulze, S., Snellings, R., Telesca, A., Thomas, M., Vargas, F., Vollpracht, A., Walkley, B., Winnefeld, F., Ye, G., Zhang, S., Scrivener, K.. Report of RILEM TC 267-TRM phase 2: optimization and testing of the robustness of the R3 reactivity tests for supplementary cementitious materials,Materials and structures (2022), Vol. 55, DOI 10.1617/s11527-022-01928-6

Benhelal, Emad and Shamsaei, Ezzatollah and Rashid, Muhammad Imran,Challenges against CO2 abatement strategies in cement industry: A review, Journal of environmental sciences (2011), Vol. 104, pp. 84-101, DOI 10.1016/j.jes.2020.11.020.

Bernal, S. A., Rodríguez, E. D., Kirchheim, A. P., & Provis, J. L. Management and Valorization of wastes through use in producing alkali-activated cement materials. Journal of Chemical Technology & Biotechnology (2016). Vol. 91(9), p. 2365-2388, DOI 10.1002/jctb.4927

Biddau, R. and Cidu, R. and Da Pelo, S. and Carletti, A. and Ghiglieri, G. and Pittalis, D.Source and fate of nitrate in contaminated groundwater systems: Assessing spatial and temporal variations by hydrogeochemistry and multiple stable isotope tools, sicence of the total environment (2019), Vol.647, p. 1121-1136, DOI 10.1016/j.scitotenv.2018.08.007

Chaipanich, Arnon and Thongsomboon, Supitchaya and Chomyen, Phakin,Thermogravimetric analysis and phase characterizations of Portland fly ash limestone cements, Journal of thermal analysis and calorimetry (2020) . Vol. 142, p. 183-190 ,DOI = 10.1007/s10973-020-10016-2

Contreras, M., Teixeira, S.R., Lucas, M.C., Lima, L.C.N., Cardoso, D.S.L., da Silva, G.A.C.,Gregorio, G.C., de Souza, A.E., dos Santos, A., 2016. Recycling of construction and demolition waste for producing new construction material (Brazil case-study). Construct. Build. Mater. 123, 594e600. https://doi.org/10.1016/ J.CONBUILDMAT.2016.07.044.

Coumou, Dim and Rahmstorf, Stefan, A decade of weather extremes, Nature climate change (2012), Vol. 1, p. 491-496, DOI 10.1038/NCLIMATE1452

De Grazia, M. T. and Sanchez, L. F. M. and Yahia, A. Towards the design of eco-efficient concrete mixtures: An overview, Journal of cleaner production (2023),Vol. 389, DOI 10.1016/j.jclepro.2022.135752

Ding, Wenwen and He, Yongjia and Lu, Linnu and Wang, Fazhou and Hu,Shuguang,Comparative study of hydration of monocalcium aluminate and quaternary phase and the amorphous AH(3)phase in their hydrates, Journal of thermal analysis and calorimetry (2020), Vol. 141, p. 707-716, DOI 10.1007/s10973-019-09069-9

Donatello, Shane and Kuenzel, Carsten and Palomo, Angel and Fernandez-Jimenez, Ana, High temperature resistance of a very high volume fly ash cement paste, Cement\& concrete composites (2014), Vol. 45, p. 234-242, 10.1016/j.cemconcomp.2013.09.010

Estadisticas gestor de residuos en catalunya,13/05/2023, http://estadistiques.arc.cat/ARC/estadistiques/Informe_DARIG_2021.pdf

Falzone, Gabriel and Balonis, Magdalena and Sant, Gaurav, X-AFm stabilization as a mechanism of bypassing conversion phenomena in calcium aluminate cements,Cement and concrete research (2015), Vol. 72, p. 54-68, DOI 10.1016/j.cemconres.2015.02.022

Friedlingstein, Pierre and Jones,Global Carbon Budget 2021,Earth system science data(2022), Vol.14, DOI 10.5194/essd-14-1917-2022

Gastaldi, D. and Canonico, F. and Capelli, L. and Buzzi, L. and Boccaleri, E. and Irico, S. An investigation on the recycling of hydrated cement from concrete demolition waste, Cement\& concrete composites, Vol. 61, p. 29-35, DOI 10.1016/j.cemconcomp.2015.04.010

Julien Bizzozzero, Karen L. Scrivener. Limestone reaction in calcium aluminate cement-calcium sulfates systems. Cement and concrete research, 2015, Vol. 76, p 159-169. http://doi.org/10.1016/j.cemconres.2015.05.019.

Liu, Qiong and Tong, Teng and Liu, Shuhua and Yang, Dezhi and Yu, Qiang, Investigation of using hybrid recycled powder from demolished concrete solids and clay bricks as a pozzolanic supplement for cement, Construction and building materials (2014), Vol. 73, p.754-763, DOI = 10.1016/j.conbuildmat.2014.09.066

Marklund, Erik and Andreas, Lale and Lagerkvist, Anders, Float-sink separation of construction and demolition waste fines, Detritus (2018), Vol. 3, p. 13-18, DOI 10.31025/2611-4135/2018.13648

Marvila, M., de Matos, P., Rodríguez, E., Monteiro, S. N., de Azevedo, A. R. Recycled aggregate: a viable solution for sustainable concrete production. *Materials* (2022), Vol. *15*(15), p. 5276, DOI 10.3390/ma15155276

Matschei, T. and Lothenbach, B. and Glasser, F. P. The role of calcium carbonate in cement hydration, Cement and concrete research (2007), Vol. 37, p.551-558, DOI = 10.1016/j.cemconres.2006.10.013

Meyer, C. The greening of the concrete industry, Cement\& concrete composites (2009), Vol. 31, p. 601-605, DOI 10.1016/j.cemconcomp.2008.12.010

Ministerio de Industria y comercio, Estadística del cemento serie histórica 1992-2021, [Consulta:17/05/2023}https://industria.gob.es/es-es/estadisticas/Paginas/Estadistica-Cemento.aspx

Moropoulou, A and Bakolas, A and Bisbikou, K, Characterization of ancient, Byzantine and later historic mortars by thermal and X-ray diffraction techniques, Thermochimica acta(1995), Vol 269, p. 779-795, DOI 10.1016/0040-6031(95)02571-5

Programa General de gestión de residuos y recursos de catalunya 2013-2020 (PRECAT20), obtain from "residu gencat" by the 01/06/2023, source: https://residus.gencat.cat/web/.content/home/ambits_dactuacio/planificacio/precat20/precat20_web_cast.pdf

Ramanathan, Sivakumar and Croly, Michael and Suraneni, Prannoy, Comparison of the effects that supplementary cementitious materials replacement levels have on cementitious paste properties , Cement\& concrete composites (2020), Vol. 112, DOI 10.1016/j.cemconcomp.2020.103678

Schimel, DS, Terrestrial Ecosystems and the carbon-cycle, Global change biology(1995), Vol. 1, p. 77-91, DOI 10.1111/j.1365-2486.1995.tb00008.x

Skibsted, Jurgen and Snellings, Ruben, Reactivity of supplementary cementitious materials (SCMs) in cement blends, Cement and concrete research (2019), Vol. 124, DOI 10.1016/j.cemconres.2019.105799

Sousa, V., Bogas, J. A., Real, S., Meireles, I. Industrial production of recycled cement: Energy consumption and carbon dioxide emission estimation. *Environmental science and pollution research(2023)*, Vol. *30*(4), p. 8778-8789, DOI 10.1007/s11356-022-20887-7

Tang, Qin and Ma, Zhiming and Wu, Huixia and Wang, Wan, The utilization of eco-friendly recycled powder from concrete and brick waste in new concrete: A critical review, Cement\& concrete composites (2020), Vol. 114, DOI 10.1016/j.cemconcomp.2020.103807

Turner, Louise K.; Collins, Frank G.Carbon dioxide equivalent (CO2-e) emissions: A comparison between geopolymer and OPC cement concrete (2013), Construction and building materials, 43, pp. 125 - 130, DOI: 10.1016/j.conbuildmat.2013.01.023

Wu, Huixia and Hu, Ruihan and Yang, Dingyi and Ma, Zhiming, Micro-macro characterizations of mortar containing construction waste fines as replacement of cement and sand: A comparative study,Construction and building materials (2023), Vol. 383, DOI 0.1016/j.conbuildmat.2023.131328

Yang, Jun and Zhang, Wei and Hou, Dongshuai and Zhang, Gaozhan and Ding, Qingjun, Structure, dynamics and mechanical properties evolution of calcium silicate hydrate induced by dehydration and dihydroxylation , Construction and building materials (2021), Vol. 291, DOI 10.1016/j.conbuildmat.2021.123327

Yuelin Li, Samuel Eyley, Wim Thielemans, Qiang Yuan, Jiabin Li, Valorization of deep soil mixing residue in cement-based materials, Resources, Conservation and Recycling (2022), Vol.187 ,https://doi.org/10.1016/j.resconrec.2022.106597.

Zhang, Dongsheng and Zhang, Shuxiang and Huang, Bowen and Yang, Qiuning and Li, Jiabin, Comparison of mechanical, chemical, and thermal activation methods on the utilisation of recycled concrete powder from construction and demolition waste, Journal of building engineering (2022), Vol. 61, DOI 10.1016/j.jobe.2022.105295

Zhang, Qi and Ye, Guang, Dehydration kinetics of Portland cement paste at high temperature, Journal of thermal analysis and calorimetry (2019), Vol. 110, p. 153-158, DOI 10.1007/s10973-012-2303-9

Zhutovsky, Semion and Shishkin, Andrei, Recycling of hydrated Portland cement paste into new clinker, Construction and building materials (2021), Vol. 280, DOI 10.1016/j.conbuildmat.2021.122510

Annexes

Annex 1: Table by residual code, showing entries(E) and exits (S) of waste and it's wt%.

Categoria	Entrada (t)	Salida (t)	E-S	Wt%
RESIDUS DE LA PROSPECCIÓ, EXTRACCIÓ DE MINES I CANTERES I TRACTAMENTS FÍSICS I QUÍMICS DE MINERALS	1.073,98	643,74	430,24	0,00
RESIDUS DE L'AGRICULTURA, HORTICULTURA, AQÜICULTURA, SILVICULTURA, CAÇA I PESCA; RESIDUS DE LA PREPARACIÓ I ELABORACIÓ D'ALIMENTS	1.307.141,05	67.260,92	1.239.880,13	8,13
RESIDUS DE LA TRANSFORMACIÓ DE LA FUSTA I DE LA PRODUCCIÓ DE TAULERS I MOBLES, PASTA DE PAPER, PAPER I CARTRÓ	257.157,61	290.905,27	-33.747,66	-0,22
RESIDUS DE LES INDÚSTRIES DEL CUIR, DE LA PELL I DEL TÈXTIL	25.946,77	9.244,10	16.702,67	0,11
RESIDUS DE LA REFINACIÓ DEL PETROLI, PURIFICACIÓ DEL GAS NATURAL I TRACTAMENT PIROLÍTIC DEL CARBÓ	426,78	25,08	401,70	0,00
RESIDUS DE PROCESSOS QUÍMICS INORGÀNICS	46.186,80	4.064,75	42.122,05	0,28
RESIDUS DE PROCESSOS QUÍMICS ORGÀNICS	309.224,96	47.800,81	261.424,15	1,71
RESIDUS DE LA FABRICACIÓ, FORMULACIÓ, DISTRIBUCIÓ I UTILIT)ACIÓ ;FFDUJ DE REVESTIMENTS, ADHESIUS, SEGELLANTS I TINTES D'IMPRESSIÓ	33.701,10	13.781,77	19.919,33	0,13
RESIDUS DE LA INDÚSTRIA FOTOGRÀFICA	958,43	480,35	478,08	0,00
RESIDUS DE PROCESSOS TÈRMICS	428.926,21	384.308,40	44.617,81	0,29
RESIDUS DEL TRACTAMENT QUÍMIC DE SUPERFÍCIE I DEL RECOBRIMENT DE METALLS I ALTRES MATERIALS; RESIDUS DE LA HIDROMETAL·LÚRGIA NO FÈRRIA	41.306,60	4.914,83	36.391,77	0,24
RESIDUS DE L'EMMOTLLAMENT I TRACTAMENT FÍSIC I MECÀNIC DE SUPERFÍCIE DE METALLS I PLÀSTICS	277.668,08	56.311,51	221.356,57	1,45
RESIDUS D'OLIS I DE COMBUSTIBLES LÍQUIDS	180.941,53	39.627,35	141.314,18	0,93
RESIDUS DE DISSOLVENTS, REFRIGERANTS I PROPEL·LENTS ORGÀNICS	13.974,75	9.837,42	4.137,33	0,03
RESIDUS D'ENVASOS; ABSORBENTS, DRAPS DE NETEJA; MATERIALS DE FILTRACIÓ I ROBA DE PROTECCIÓ NO ESPECIFICATS EN CAP ALTRA CATEGORIA	770.337,97	187.369,26	582.968,71	3,82
RESIDUS NO ESPECIFICATS EN CAP ALTRE CAPÍTOL DE LA LLISTA	996.760,10	319.407,11	677.352,99	4,44
RESIDUS DE LA CONSTRUCCIÓ I DEMOLICIÓ	7.258.018,92	1.051.573,42	6.206.445,50	40,69
RESIDUS DE SERVEIS MÈDICS O VETERINARIS O D'INVESTIGACIÓ ASSOCIADA	101.348,06	5.995,68	95.352,38	0,63
RESIDUS DE LES INSTAL·LACIONS PER AL TRACTAMENT DE RESIDUS, DE LES PLANTES EXTERNES DE TRACTAMENT D''AIGÜES RESIDUALS I DE LA PREPARACIÓ D'AIGUA PER A CONSUM HUMÀ I D'AIGUA PER A ÚS INDUSTRIAL	5.639.379,04	5.296.153,53	343.225,51	2,25
RESIDUS MUNICIPALS, INCLOSES LES FRACCIONS RECOLLIDES DE MANERA SELECTIVA	7.144.482,20	1.790.559,68	5.353.922,52	35,10
Total	24.834.960,94	9.580.264,98	15.254.695,96	100,00

Annex 2.

Historical data of the cement industry in Catalunya (1992-2021)

Year	Cement production	Apparent consume
1992	4,035,834	3,642,240
1993	3,923,374	3,016,921
1994	4,616,419	3,150,425
1995	4,956,851	3,374,071
1996	4,707,011	3,291,885
1997	5,280,785	3,703,428
1998	6,270,750	4,352,444
1999	6,658,274	4,921,267
2000	6,734,064	5,306,204
2001	7,363,366	5,782,474
2002	7,897,027	6,484,405
2003	8,034,400	6,833,619
2004	8,378,356	7,129,975
2005	8,887,867	7,477,903
2006	9,470,297	8,668,491
2007	9,604,339	8,814,062
2008	7,003,805	6,779,070
2009	5,223,182	4,719,534
2010	5,110,303	3,775,600
2011	4,069,060	3,045,558
2012	3,024,038	2,124,661
2013	2,104,112	1,585,673
2014	2,355,427	1,454,988
2015	2,403,932	1,544,664
2016	2,653,309	1,591,715
2017	3,174,892	1,852,124
2018	2,601,170	1,819,490
2019	3,294,718	2,234,791
2020	3,074,595	1,999,763
2021	3,348,705	2,219,457
Total Result	**156,260,262**	**122,696,903**

Annex 3.

DTA/TG of FCG material.

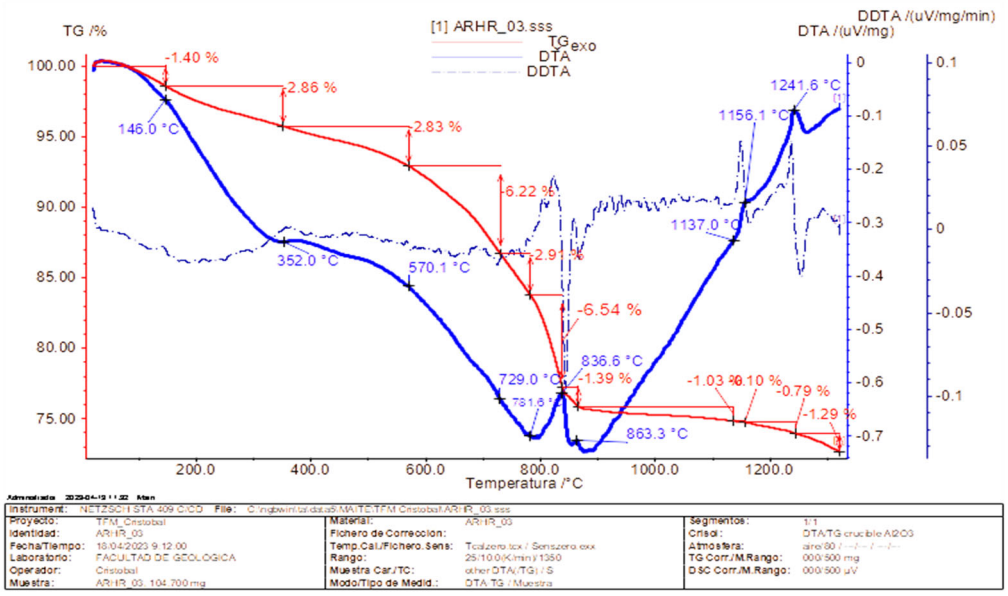

Instrument:	NETZSCH STA 409 C/CD	File:	C:\ngbwin\tzl-data\5.MA\TG\TFM Cristobal\ARHR_03.sss		
Proyecto:	TFM_Cristobal	Material:	ARHR_03	Segmentos:	1/1
Identidad:	ARHR_03	Fichero de Correccion:		Crisol:	DTA/TG crucible Al2O3
Fecha/Tiempo:	18/04/2023 9:12:00	Temp.Cal./Fichero.Sens:	Tcal.zero.tcx / Sens.zero.exx	Atmosfera:	aire/80 / --- / --- / ---
Laboratorio:	FACULTAD DE GEOLOGICA	Rango:	25/1000/K/min/1350	TG Corr./M.Rango:	000/500 mg
Operador:	Cristobal	Muestra Car./TC:	other DTA/TG / S	DSC Corr./M.Rango:	000/500 uV
Muestra:	ARHR_03, 104.700 mg	Modo/Tipo de Medid.:	DTA TG / Muestra		